

Journal of Materials Chemistry A

Accepted Manuscript



This is an *Accepted Manuscript*, which has been through the Royal Society of Chemistry peer review process and has been accepted for publication.

Accepted Manuscripts are published online shortly after acceptance, before technical editing, formatting and proof reading. Using this free service, authors can make their results available to the community, in citable form, before we publish the edited article. We will replace this *Accepted Manuscript* with the edited and formatted *Advance Article* as soon as it is available.

You can find more information about *Accepted Manuscripts* in the [Information for Authors](#).

Please note that technical editing may introduce minor changes to the text and/or graphics, which may alter content. The journal's standard [Terms & Conditions](#) and the [Ethical guidelines](#) still apply. In no event shall the Royal Society of Chemistry be held responsible for any errors or omissions in this *Accepted Manuscript* or any consequences arising from the use of any information it contains.

ARTICLE

Tuning the Band Gap of Ferritin Nanoparticles by Co-Depositing Iron with Halides or Oxo-anions

Cite this: DOI: 10.1039/x0xx00000x

Trevor J. Smith^a, Stephen D. Erickson^b, Catalina Matias Orozco^a, Andrew Fluckiger^a, Lance M. Moses^a, John S. Colton^b, Richard K. Watt^a

Received 00th January 2012,
Accepted 00th January 2012

DOI: 10.1039/x0xx00000x

www.rsc.org/

Iron-containing ferritin has been used for light harvesting and as a photocatalyst. In this study, we test the hypothesis that changing the iron mineral core composition can alter the light harvesting and photocatalytic properties of ferritin, by co-depositing iron in the presence of halides or oxo-anions. This caused the anions to be incorporated into the iron mineral. We report that some of these new iron minerals possess different band gaps than the original ferrihydrite within ferritin. We found an increase in band gap of up to 0.288 eV or a decrease by as much as 0.104 eV, depending on the type of anion and amount of anions incorporated into the ferrihydrite mineral.

ARTICLE

Journal Name

Introduction

Nanoparticles (<100 nm) have high photon-exciton conversion efficiencies, which are especially desirable in photovoltaic (PV) devices.^{1,2,3} Scientists developing multi-junction PV cells seek to surpass the theoretical efficiency limit of single junction cells⁴ by utilizing multiple layers of materials with different band gaps.^{5,6,7} The band gap dictates the minimum energy needed to excite an electron into the conduction band, and the amount of useful energy that can be extracted from each excitation. For increased efficiency, each layer must have a greater band gap than the layer below it, reducing the energy lost to heat. However, current methods have only produced a handful of compatible materials,⁵ thus severely limiting the ability to develop multi-junction solar cells because of the limited range of materials with the desired band gaps.

The development of multi-junction PV cells with nanoparticles will require: 1) methods to synthesize a library of nanoparticles with the appropriately tuned band gaps; and 2) methods to deposit the nanoparticles in ordered arrays in layers. Ferritin was recently identified as model molecule for PV systems because of its unique properties as a hybrid organic/inorganic photocatalyst.⁸ In this study we describe our efforts to design a library of ferritin iron-containing nanoparticles with altered band gaps that can be used in multi-junction PV cells.

Ferritin is the iron storage protein found in virtually every organism. It is a spherical biomolecule measuring 12 nm in diameter with an 8 nm hollow interior and is composed of 24 polypeptide subunits.⁹ These subunits form an extremely stable protein complex that is capable of withstanding a pH range of 4-12 and maintain conformation up to 85 °C.¹⁰ Ferritin is shown in Figure 1A.

Ferritin binds and mineralizes iron and sequesters it inside the 8 nm diameter protein cage as an iron oxide nanoparticle (Fig. 1B). The protein is capable of holding up to 4500 iron atoms as an $\text{Fe}_2\text{O}_3 \cdot 0.5\text{H}_2\text{O}$ or ferrihydrite mineral (often written as $\text{Fe}(\text{O})\text{OH}$ for convenience).¹¹

The iron mineral can be removed from ferritin by chemical reduction and chelation, producing an empty protein nanocage.²⁵ The iron core can be reconstituted by adding iron to the empty protein shell (Fig. 2A).²⁵ Additionally, non-naturally occurring minerals can be synthesized inside ferritin by a variety of synthetic methods using different metals (Ti, Cr, Mn, Fe, Co, Ni, Cu, Eu and U) and anions (S , Se , PO_4^{3-} , AsO_4^{3-} , VO_3^- , MoO_4^{2-} , WO_4^{2-}).^{8,12,13,14,15} Therefore, a library of ferritin nanoparticle materials is available to be studied.

The protein shell of ferritin also provides unique handles for materials science applications. For instance, the protein shells of ferritin will self-assemble on surfaces such as silica or gold in hexagonally close packed arrays.¹⁶ Additionally, the organic shell can be functionalized and organized in architectures of 2- and 3-dimensional structures.^{17,18} The ability to assemble ferritin and its encapsulated mineral in ordered arrays and layers, particularly on transparent electrode surfaces such as indium tin oxide electrodes¹⁹, makes ferritin an appealing substrate for multi-junction PV cells.

Upon illumination, ferritin absorbs light, creating excitons where the excited electrons have been used to reduce a variety of species (Au ,²⁰ Cr ,²¹ Cu ,²² Cytochrome c and Viologens²³). Nikandrov demonstrated that the light absorption takes place in the ferrihydrite core, a semiconducting material whose band gap has been reported by several groups.^{20, 21, 24, 26}

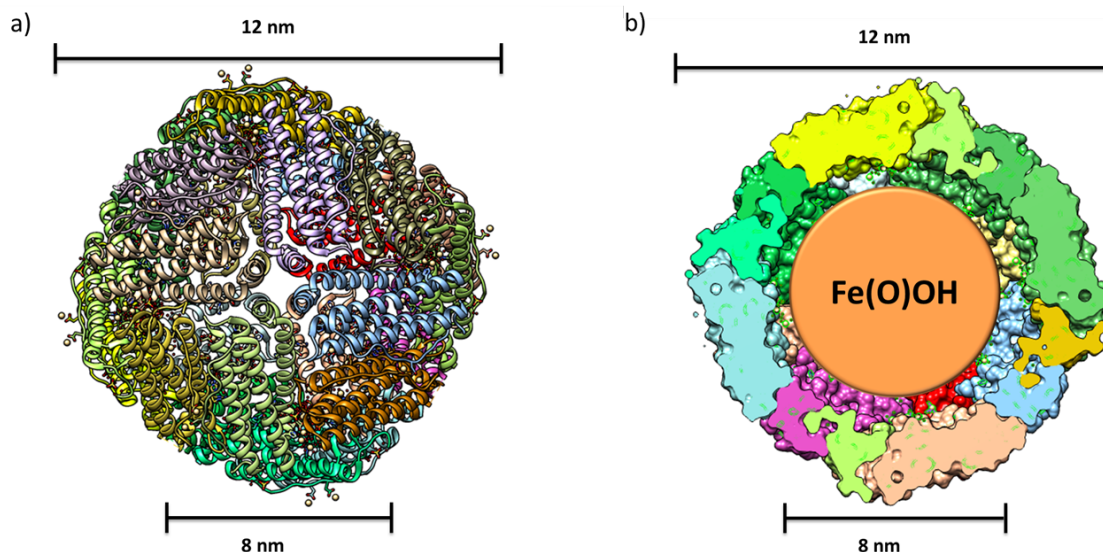


Figure 1 – Ferritin protein. a) A ribbon diagram of the protein shell of Ferritin with the four-fold channel in the center. b) Cross-section of ferritin with a representative ferrihydrite core in the center. Figures generated using Chimera code PDB 1fha.

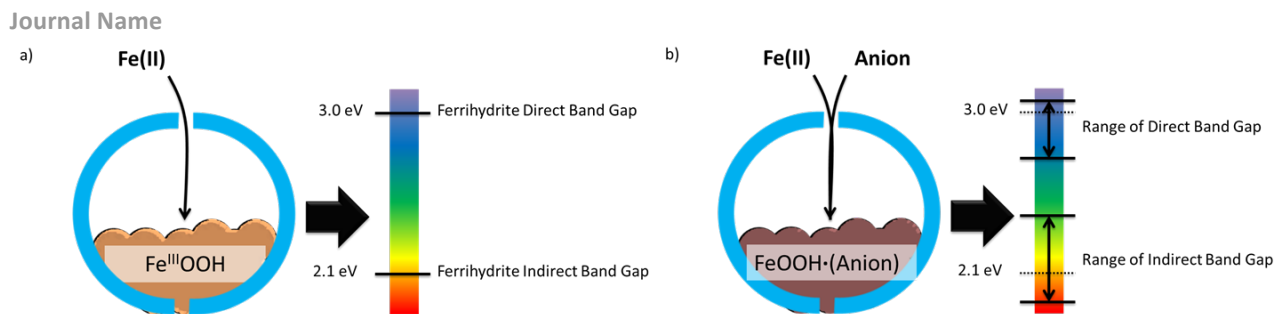


Figure 2- Scheme of band gap alterations using anion deposition in ferritin. a) The natural ferrihydrite mineral band gap is shown on a color scale, with the direct and indirect band gap energies. b) An anion co-deposited iron core, showing the extent of band gap variation possible by co-depositing various anions. The direct and indirect band gaps from Figure 2a are shown as a dotted line.

Recently, Colton et al.²⁶ used Optical Absorption Spectroscopy (OAS) to establish the native ferrihydrite mineral in ferritin as an indirect band gap semiconductor, and accurately measured an indirect band gap at 2.140 ± 0.010 eV (579.7 nm), a direct transitions (sometimes called a direct band gap) at 3.053 ± 0.005 eV (406.1 nm), and a defect-related state having a binding energy of 0.220 ± 0.010 eV.

The ability to synthesize artificial minerals inside ferritin expands the potential light harvesting materials that can be prepared. In this paper, we study altered iron-containing ferritin minerals. Polanams et al.¹⁴ were able to co-deposit oxo-anions into the ferrihydrite mineral during iron loading, and reported that co-deposition changed the iron loading kinetics. The UV/Vis absorption spectrum of each of these ferritin iron/oxo-anions complexes was different, indicating changes to the mineral and the band gap of each mineral. Hilton et al.²⁵ were able to reduce the ferrihydrite mineral in the presence of different anions to create an Fe(X)OH core, where the symbol X in the chemical formula represents halides or oxo-anions. The ferritin solution went from a red-orange color to a pale yellow as the iron was reduced from Fe^{III} to Fe^{II}. This significant color change is indicative of a change in band gap. Based on these observations, Colton et al.²⁶ tested the effect of halides that associated with the surface of the iron mineral in ferritin and observed that halides slightly altered the band gaps of the ferrihydrite mineral.

In this study, we test the hypothesis that the co-deposition of iron and anions into ferritin alters the band gap of the new iron mineral in ferritin. We synthesized and characterized these new anion-containing iron minerals formed in ferritin and employed OAS to measure the band gaps of these ferritins. We report new band gap energies for these new ferritin minerals and compare them to the natural iron core (ferrihydrite) of ferritin. Figure 2B schematically represents how the minerals were synthesized and represents that an altered band gaps were observed.

Experimental

Apo-ferritin was prepared by removing the iron from horse spleen ferritin (Sigma-Aldrich CAS# F4503) using established methods.^{14,27} Native ferritin was dialyzed against thioglycolic acid and 0.050 M tris(hydroxymethyl)aminomethane (TRIS) to remove all iron from ferritin. The resulting iron free ferritin was then dialyzed against Milli-Q water in 0.10% bicarbonate buffer at pH 7.4. Further dialysis was used to exchange ferritin into imidazole buffer.

Reconstituted ferrihydrite cores with no anions present were made by adding iron to an iron free ferritin solution (5 mg/mL, 1.11×10^{-5} M) in an imidazole buffer (prepared at 1M pH 7.4) with a final volume of 1.5 mL. The pH of the solution was kept at pH 7.4 by careful titration with NaOH. We have observed an aging effect where the measured band gap slowly changes with time (several hours to 1 day) immediately after the synthesis of a new core. This aging effect is presumably due to the reorganization of the mineral to its most stable state. For this study, all cores were aged for 5 days, far longer than was necessary, to be sure the mineralization process was complete. The mineral core synthesis was performed by adding 10 mM ferrous ammonium sulfate prepared in 10 mM nitric acid at a rate no greater than 100 irons per ferritin per 10 minutes. The pH was maintained at 7.4 by adding NaOH to neutralize acid produced from iron mineralization. Core sizes were selected between 500-2000 Fe/ ferritin.

Co-deposition of halides was achieved by loading iron into ferritin using the same method as above, but preparing the buffer solution with 200 mM concentrations of the desired sodium halide salt (except for fluoride, which was kept at 1 mM due to significant inhibition of iron loading with the higher fluoride concentrations).

Co-deposition of oxo-anions was performed by adding iron into a ferritin solution containing 1 mM sodium oxo-anion. Additional samples with higher oxo-anion concentrations of 5 mM oxo-anion were prepared by simultaneous additions in separate injections of 100 mM oxo-anion and 100 mM ferrous ammonium sulfate prepared in 10 mM nitric acid, at a rate no greater than 50 irons per 10 minutes up to a targeted bulk state (>900 Fe/ferritin). The pH was maintained at 7.4 by titration with 300 mM sodium hydroxide. All samples were mixed with a BioRad P-10 slurry in a 1:1 volume ratio to remove any iron-oxo-anion polymers.²⁸ A BioRad P-10

ARTICLE

Journal Name

slurry solution was mixed on a rocking platform for at least 30 min and then centrifuged and the ferritin supernatant was decanted. The decanted iron-polymer free solutions were then passed over a Sephadex G-75 desalting column with 50 mM pH 7.4 imidazole buffer.

The iron content of each sample was determined by treating the ferritin samples with bypyridine and dithionite and measuring the iron-bipyridine absorbance at 522 nm ($\epsilon_{522}=8650 \text{ M}^{-1} \text{ cm}^{-1}$).²⁹ The protein content was measured by the Lowry method,³⁰ and a ratio between the iron and protein concentration gave the relative Fe/ferritin ratio.

The halides and phosphate which were co-deposited into the ferrihydrite mineral cores were measured using Orion Ion Selective Electrodes (ISE), and additional elemental analysis was performed using inductively coupled plasma-mass spectrometry (ICP-MS) for all oxo-anion samples.

Band gaps were measured by optical absorption spectroscopy using a setup as described by Colton et al.²⁶ All samples were prepared and allowed to stabilize for 5 days after core remineralization to insure a stable mineral for band gap measurements.

Transmission Electron Microscopy (TEM) images were taken of all samples using a Tecnai F30 in parallel imaging mode. Energy Dispersive X-ray (EDX) spectrometry was conducted with an EDAX attached to a Tecnai F20 TEM. ImageJ was used to measure core size using an average of over 80 cores per sample. A representative figure of the TEM analysis is shown in Figure 3 with the data for all other

samples available in the supplemental data section of the paper.

Results and Discussion

Sample Characterization

The newly synthesized ferritin cores that contained co-deposited anions were characterized to determine the extent of anion incorporation in the minerals. First, we performed TEM to confirm that the iron and anions were actually deposited inside the ferritin interior. TEM analysis of the samples showed nanoparticles of $\sim 9 \text{ nm}$ diameter (Fig. 3A) consistent with the size of the ferritin interior. Negative staining of the samples showed that these nanoparticles were present inside the ferritin protein shell (Fig 3B). EDX analysis also showed the expected composition of iron and the appropriate anion in the mineral analysis (Fig. 3C shows representative data for the iron molybdate ferritin sample). The TEM analysis of the other ferritin samples is presented in the supplemental data section. The silicon and copper peaks are from the silicon detector in the instrument, and the copper grids used to image the ferritin samples, respectively. Additional elemental analysis of the samples was performed to determine the amount of the anions deposited in ferritin by using ion-selective electrodes (ISEs) and ICP-MS. These results are summarized in Table 1.

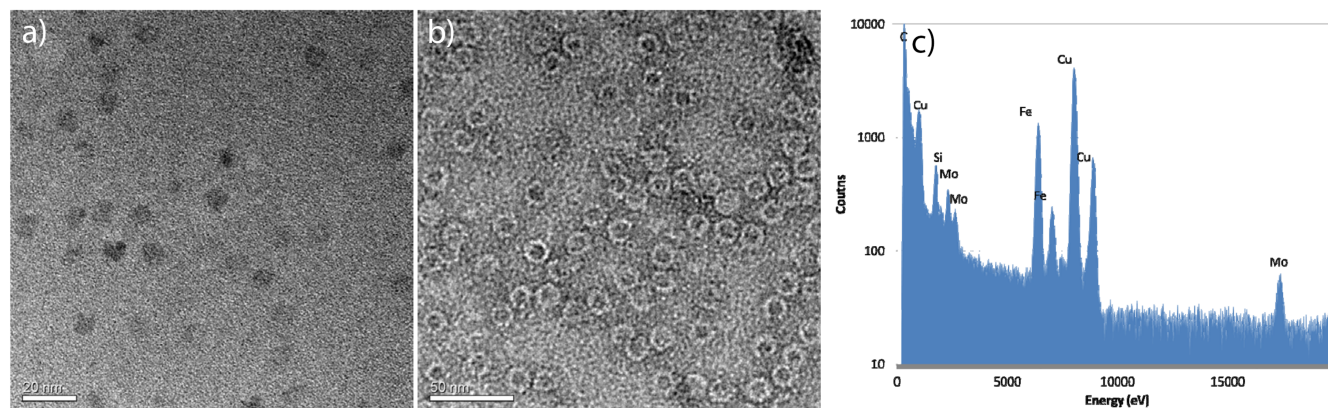


Figure 3 – TEM images and EDX analysis of ferritin containing co-deposited iron and MoO_4^{2-} . a) Unstained TEM image of ferritin with an iron and molybdate core ($\text{Fe(O)OH}\cdot(\text{MoO}_4)$). b) Uranyl acetate stained iron and molybdate ferritin sample showing protein with the mineral core inside. c) EDX analysis from TEM showing molybdenum and iron content from Figure 3a. Additional figures for each anion co-deposited sample can be seen in the supplemental data.

| Co-deposition Anion | Iron per Ferritin | Anion per Ferritin | Core Size (nm) | Indirect Band Gap (eV) | Change in Indirect (eV) | Direct Band Gap (eV) | Change in Direct (eV) |
|--------------------------------|-------------------|--------------------|----------------|------------------------|-------------------------|----------------------|-----------------------|
| No Salt – Bulk | 900 ± 71 | n/a | 9.05 ± 1.44 | 2.092 ± 0.011 | n/a | 2.992 ± 0.012 | n/a |
| Halides | | | | | | | |
| F ⁻ | 2650 ± 430 | 260 | Not measured | 2.078 ± 0.012 | -0.014 | 2.991 ± 0.008 | -0.001 |
| Cl ⁻ | 2090 ± 280 | 210 | 9.11 ± 0.92 | 2.077 ± 0.012 | -0.015 | 2.974 ± 0.010 | -0.018 |
| Br ⁻ | 2400 ± 250 | 240 | 9.25 ± 0.55 | 2.032 ± 0.012 | -0.060 | 2.942 ± 0.016 | -0.050 |
| I ⁻ | 2600 ± 300 | 260 | 9.33 ± 0.92 | 2.050 ± 0.012 | -0.042 | 2.934 ± 0.014 | -0.058 |
| 1 mM Oxo-Anion | | | | | | | |
| PO ₄ ³⁻ | 2000 ± 400 | 185 ± 20 | Not measured | 2.139 ± 0.010 | 0.047 | 3.009 ± 0.008 | 0.017 |
| MnO ₄ ²⁻ | 2000 ± 300 | 75 ± 1 | Not measured | 2.080 ± 0.010 | -0.012 | 2.994 ± 0.008 | 0.002 |
| MoO ₄ ²⁻ | 1175 ± 200 | 95 ± 2 | Not measured | 2.116 ± 0.012 | 0.024 | 2.990 ± 0.010 | -0.002 |
| WO ₄ ²⁻ | 1750 ± 100 | 1000 ± 10 | Not measured | 2.215 ± 0.012 | 0.123 | 3.058 ± 0.008 | 0.066 |
| 5 mM Oxo-Anion | | | | | | | |
| PO ₄ ³⁻ | 430 ± 53 | 60 ± 5 | Not measured | 2.380 ± 0.024 | 0.288 | 3.231 ± 0.014 | 0.239 |
| MnO ₄ ²⁻ | 127 ± 24 | 112 ± 1 | 8.38 ± 0.67 | 1.988 ± 0.012 | -0.104 | 2.878 ± 0.010 | -0.114 |
| MoO ₄ ²⁻ | 1075 ± 140 | 345 ± 3 | 8.58 ± 0.81 | 2.113 ± 0.010 | 0.021 | 3.001 ± 0.010 | 0.009 |
| WO ₄ ²⁻ | 1060 ± 120 | 1430 ± 10 | 8.26 ± 1.01 | 2.242 ± 0.010 | 0.150 | 3.062 ± 0.012 | 0.070 |

Table 1. Reported metals per ferritin, anion co-deposition, and band gap values. It should be noted that the 1 mM and 5 mM titles are for the concentration of oxo-anions used during synthesis, and not the actual concentration of the anions present inside the ferritin protein. The "Change in Indirect" and "Change in Direct" columns indicate the variation in band gap relative to the "No Salt – Bulk" values. Also see Figure 4, 5, and 6.

ARTICLE

Effect of Core Size

Previously, Colton et al.²⁶ demonstrated a quantum confinement effect where smaller ferritin cores possessed a larger band gap than larger ferritin cores. As we initiated studies on these new ferritin cores with co-deposited anion and iron cores we recognized the importance of evaluating if these new samples exhibited any quantum confinement effects. Figure 4 shows that small cores do have larger band gaps, however, when the core sizes exceeded 900 irons per ferritin, a “bulk-like” state was observed where the band gap no longer varies with size. By defining the “bulk-like” state as cores >900 Fe/ferritin we were able to define deviations from the ferrihydrite band gap as being due to the co-deposition of the anions and not due to quantum confinement effects. Any changes in band gap mentioned in this manuscript will be in relation to this “bulk-like” state.

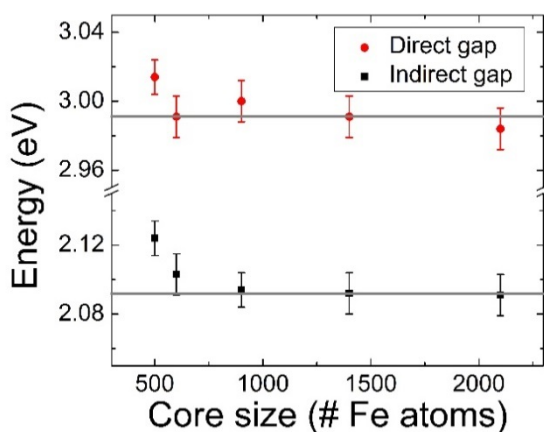


Figure 4. Reconstituted ferrihydrite cores with no anions present. The gray lines show the band gap of bulk-like Nano crystals.

Effect of Halides

Halides were successfully deposited into the ferrihydrite mineral as shown in Table 1. These minerals were synthesized in the presence of 200 mM halide concentrations to allow for a greater probability that an anion would co-deposit with iron during mineralization into ferritin. Colton et al.²⁶ showed that adsorbing halides to the ferrihydrite surface using salts in solution slightly lowered the indirect band gap, by about 0.010-0.020 eV, but increased the direct band gap (0.010 to 0.050) [See reference 26, Figure 5]. We tested the hypothesis that anion co-deposition inside the mineral would further alter the band gap of these iron/halide minerals. ISE analysis showed

that approximately one halide per ten iron ions was found in the new ferritin mineral (Table 1). Anion co-deposition with iron was accompanied by a decrease in band gap (Table 1), particularly for Br⁻ and I⁻. The band gap changes were much more profound for the co-deposited halides than the surface adsorbed halides [See reference 26, Figure 5]. The results show that anions deposited in the mineral core lowered the direct band gap by as much as 0.058 eV in the case of I⁻, and the indirect band gap by 0.060 eV in the case of Br⁻ (Fig. 5, Table 1).

Effect of Oxo-Anions

Ferritin iron cores were synthesized with oxo-anions following the method of Polanams et al.¹⁴ These samples also showed variations in the band gap compared to the ferritin ferrihydrite control (Fig. 6, Table 1). Ferritin oxo-anion samples were prepared using two different oxo-anion concentrations during synthesis, namely 1 mM and 5 mM. This allowed us to study alterations to the band gap in preparation of ferritin minerals with different iron to oxo-anion ratios (See total oxo-anions deposited in mineral cores with different synthesis concentration, 1 mM or 5 mM in Table 1). We will refer to these distinct samples as the 1 mM and 5 mM samples throughout the rest of the manuscript, however these concentrations do not refer to the actual amount of oxo-anion incorporated, they refer to the synthesis conditions. The actual oxo-anion concentration present in the sample is indicated in Table 1. These different synthesis concentrations were chosen because it is known that some oxo-anions form polymers with iron in solution and inhibit the iron loading process into ferritin.³¹ By varying these synthesis conditions we were able to prepare ferritins with different iron to oxo-anion ratios. We removed the iron oxo-anion polymeric complex from solution so that only the ferritin samples containing iron and oxo-anions were studied for band gap measurements.

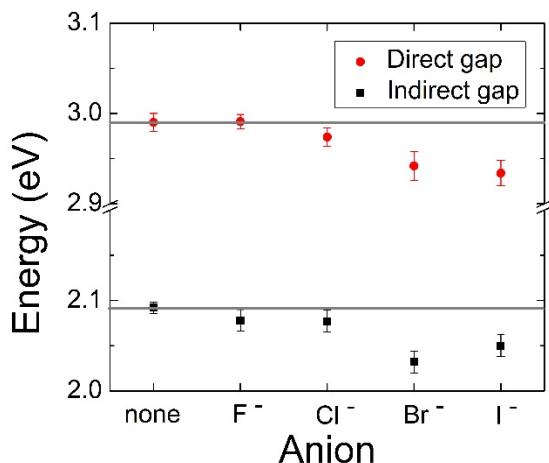


Figure 5. Band gap measurements of ferritin minerals synthesized by co-depositing iron and halides. The gray lines correspond to the direct and indirect band gaps from the bulk ferrihydrate control. (See Table 1 for a detailed listing of core size, anion incorporation, and band gap.)

We expected approximately 10-30% oxo-anion substitution based on the results of Johnson et al,³² and Polanams et al,¹⁴ who showed that phosphate as well as other oxo-anions are able to co-deposit in reconstituted ferritin cores in ratios between 10% and 30% of the total iron content. We used BioRad P-10 slurry to filter out iron oxo-anion polymers not sequestered inside ferritin²⁵, resulting in our samples having between 15% and 30% loading. As expected, the ferritin samples prepared in the presence of 5 mM oxoanions loaded a greater percentage of oxo-anions but had smaller total iron content due to complex formation outside of ferritin (Table 1). It should be noted that phosphate inhibits iron loading into ferritin, and would account for the low iron loading in the 5 mM sample.³³

The 1 mM PO₄³⁻ sample prepared in this study had 2000 iron atoms per ferritin with approximately 10% phosphate. We report a direct band gap of 3.009 eV and an indirect band gap of 2.139 eV. The iron/phosphate ratio in this synthetic core is similar to native ferritin isolated from horse spleen. Colton et al.²⁶ studied a native ferritin sample with an iron core of 1100 iron/ferritin with 10 % phosphate. Colton²⁶ reported a direct band gap value of 3.053 eV and an indirect band gap of 2.140 eV. Comparison of these two samples showed good agreement (Fig. 6, Table 1).

As expected, the ferritin sample prepared in the 5 mM phosphate solution produced a much smaller iron core (Table 1). The band gap of the sample prepared in the presence of 5 mM phosphate had a 0.288 eV increase in indirect band gap versus the bulk iron state (Fig. 6, Table 1). This change in band gap is a combination of two influencing factors. The first is the quantum confinement effect due to the small size of the 500 Fe/ferritin. If we directly compare the indirect band gap of the sample prepared in 5 mM phosphate that contains 500 Fe/ferritin (Indirect band gap = 2.380 eV) to an the iron core of

a 500 Fe/ferritin prepared in the absence of phosphate (Fig 4, Indirect band gap = 2.127) we see an increase in the band gap of 0.256 eV. However, the 500 iron/ferritin sample had a quantum confinement increase in band gap of only 0.032 eV compared to the iron ferritin sample with the “bulk state” of 900 Fe/ferritin. Therefore, the contribution to the increased band gap corresponding to the quantum confinement effect in the 500 Fe/ferritin sample containing phosphate is small compared to the influence of phosphate on the iron core.

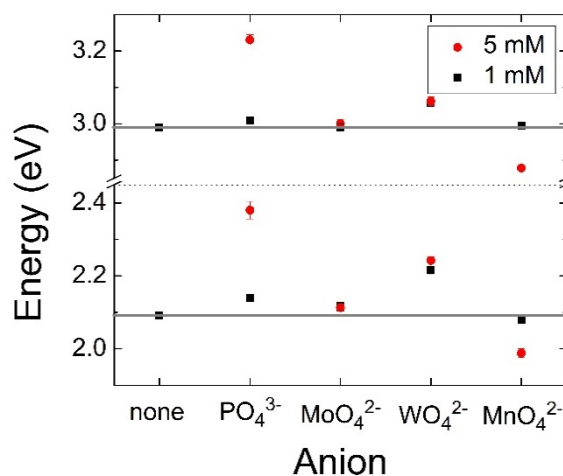


Figure 6. Ferritin samples synthesized in the presence of 1 mM oxo-anion, and ferritin samples synthesized in the presence of 5 mM oxo-anion. The gray lines correspond to the direct and indirect band gaps from the “bulk-like” ferrihydrate state. The dotted line shows a break in the y-axis separating the higher energy direct gaps from the lower energy indirect gaps. Please note that the x-axis simply denotes the anion used in the synthesis of the iron core and does not attempt to designate any other type of additional trends such as anion size, etc.

The molybdate samples did not show a significant shift in band gap (Fig. 6, Table 1). Both samples were large enough to be in the bulk-like state with 6-30% Mo loading (Table 1), but neither showed much difference in band gap, suggesting no additional benefit for PV applications by co-depositing molybdate into ferritin.

In contrast, the tungstate sample showed much higher levels of co-deposition, with tungsten to iron ratios greater than one for the 5 mM sample (Table 1). This suggests that a tungsten-iron oxide mineral was formed. Both tungstate samples had cores large enough to be in the bulk state, attributing increases in band gap to the co-deposition of the oxo-anions into the iron mineral. Both indirect and direct gaps showed increases in the band gaps, with greater increases in band gap from the greater molybdate co-deposition (Fig. 6). Specifically, the 1 mM sample showed increases of 0.123 eV for the indirect band gap and 0.066 eV for the direct band gap, while the 5 mM sample showed increases of 0.15 eV for the indirect band gap and 0.070 eV for the direct band gap (Figure 6, Table 1).

The use of the oxo-anion permanganate is different than the other oxo-anions used in this study because it is a potent oxidizing agent. We recognized that two possible reactions

could occur by adding permanganate with Fe(II) to the ferritin solution. The first is that the permanganate might simply become incorporated into the iron core in a similar fashion to the other oxo-anions. The second is that permanganate might act as an electron acceptor and rapidly oxidize the Fe(II) to Fe(III) during iron loading into ferritin. Additionally the lower valent manganese produced from permanganate oxidation might be co-deposited with iron inside ferritin creating a new mixed mineral phase of iron and manganese.

The 1 mM permanganate sample showed that about 8% of the core was manganese and the rest iron (2000 Fe/ ferritin). The 1 mM permanganate sample showed no significant change in either band gap outside of the error bars shown indicating the sample still possessed a “ferrihydrite-like” core.

In contrast, the 5 mM permanganate sample loaded significantly less iron (~127 Fe/ ferritin) but the resulting core was approximately 1 Fe:1 Mn. This 1:1 ratio suggests that instead of forming a ferrihydrite mineral, a new manganese-iron oxide mineral is formed. This sample decreased both the indirect band gap by 0.104 eV and the direct band gap by 0.114 eV from the ferrihydrite control. The quantum confinement effect observed for cores smaller than 900 iron/ferritin (Fig. 4) would suggest that the band gaps should increase when compared to the ferrihydrite ferritin core. In fact, the opposite effect occurred and we observed a decrease in band gap for the co-deposition of iron and manganese into the same mineral. This is clear evidence that a mineral very different from the natural ferrihydrite mineral has been formed in these samples. These results further show the strong effects of the manganese ions in influencing the mineral to produce smaller band gaps. Large minerals of the same 1:1 Fe:Mn may have even lower band gaps when the “bulk like” state is formed and the quantum confinement effect is mitigated. A future study will be conducted to better characterize this new iron-manganese oxide nano-material.

Conclusion

In this report we synthesized a variety of ferritin iron minerals co-deposited with halides or oxo-anions with the goal of perturbing the crystal lattice of the new mineral sufficiently to alter the band gap of the material. Such mineral alterations should allow the new materials different properties for light harvesting from the visible spectrum.

We report the successful synthesis and characterization of ferritin minerals that have iron and halides or iron and oxo-anions co-deposited inside the ferritin protein shell. The direct and indirect band gaps of each of these samples were measured using OAS techniques. We report quantum confinement effects for cores smaller than 900 Fe/ferritin. However, once the core reaches 900 Fe/ferritin a ‘bulk-like’ state is achieved and any alterations of the band gap are due to the new mineral phase.

Of the halides, bromide and iodide showed a significant decrease in both the direct and indirect band gap where the other halides did not alter the band gaps. Phosphate and

tungstate showed significant increases in both the direct and indirect band gaps where molybdenum did not alter either band gap. The magnitude of band gap shift was further affected by the extent of the anion/oxo-anion incorporated into the ferrihydrite mineral. In the case of permanganate the 5 mM sample, formed a new mineral as shown by 1:1 or greater manganese to iron ratio and a large decrease in band gaps. The band gap range for these new minerals spans from 2.878 eV (430.8 nm) to 3.231 eV (383.7 nm) for the direct gap, and from 1.988 eV (623.7 nm) to 2.380 eV (520.9 nm) for an indirect band gap. The new range of band gaps is represented in Figure 2b.

Notes and references

^a Department of Chemistry and Biochemistry, Brigham Young University, Provo UT 84602.

^b Department of Physics and Astronomy, Brigham Young University, Provo UT 84602

Supporting Information Available: TEM images with accompanying EDX spectra of NaBr, NaI, MnO₄²⁻, and WO₄²⁻ co-deposited ferritin, are shown as supplemental figures 1-4, respectively. Also, supplemental Table 1 shows the iron content and band gap measurements of ferritin samples ranging from 200 – 2100 iron/ferritin. This material is available free of charge via the Internet at <http://pubs.acs.org>.

- 1 Citations here in the format A. Name, B. Name and C. Name, *Journal Title*, 2000, **35**, 3523; A. Name, B. Name and C. Name, *Journal Title*, 2000, **35**, 3523.

¹ A. Nozik, *J. Inorg. Chem.* 2005, **44**, 6893.

² R. Schaller, M. Sykora, J. Pietryga, V. Klimov, *Nano Lett.* 2006, **6**, 424.

³ S.J. Kim, W. Kim, Y. Sahoo, A. Cartwright, P. Prasad, *Appl. Phys. Lett.* 2008, **92**, 031107.

⁴ W. Shockley, H. Queisser, *J. Appl. Phys.*, 1961, **32**, 510.

⁵ M. Green, K. Emery, Y. Hishikawa, W. Wart, E.D. Dunlop, *Prog. Photovolt: Res. Appl.* 2012, **20**, 12.

⁶ R. King, D. Law, K. Edmondson, C. Fetzer, G. Kinsey, H. Yoon, R. Sherif, N. Karam, *Appl. Phys. Lett.* 2007, **90**, 183516.

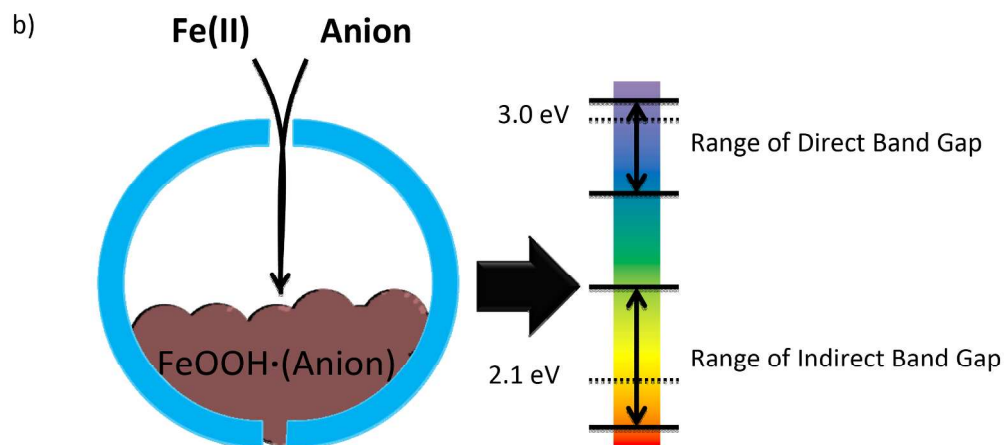
⁷ A. De Vos, *J. Phys D: Appl Phys.* 1980, **13**, 839.

⁸ R. Watt, O. Petrucci, T. Smith, *Catal. Sci. Technol.* 2013, **3**, 3103.

⁹ D. Lawson, *et al. Nature.* 1991, **349**, 541.

¹⁰ M. Hoppler, A. Schönbacher, L. Meile, R. Hurrell, T. Walczyk, *J. of Nutrition.* 2008, **5**, 878.

- ¹¹ G. Ford, *et al.*, *Philosophical Transactions of the Royal Society of London. B, Bio. Sci.* 1984, **304**, 551
- ¹² T. Douglas, V. Stark, *Inorg. Chem.*, 2000, **39**, 1828.
- ¹³ N. Galvez, P. Sanchez, J. Dominguez-Vera, *Dalton Trans.* 2005, 2492.
- ¹⁴ J. Polanams, A. Ray, R. Watt, *Inorg. Chem.* 2005, **44**, 3203.
- ¹⁵ R. Watt, R. Frankel, G. Watt, *Biochemistry* 1992, **31**, 9673.
- ¹⁶ M. Tominaga, A. Ohira, Y. Yamaguchi, M. Kunitake, *Electroanalyt. Chem.* 2004, **566**, 323.
- ¹⁷ M. Li, S. Mann, *Mater. Chem.* 20040, **14**, 2260.
- ¹⁸ K. Wong, H. Colfen, N. Whilton, T. Douglas, S. Mann, *J. Inorg. Biochem.* 1999, **76**, 187.
- ¹⁹ M. Pyon, R. Cherry, A. Bjornsen, D. Zapien, *C Langmuir*, 1999, **15**, 7040.
- ²⁰ J. Keyes, R. Hilton, J. Farrer, R. Watt, *J Nanopart Res* 2011, **13**, 2563.
- ²¹ I. Kim, H. Hosein, D. Strongin, T. Douglas, *Reduction. Chem. Mater.* 2002, **14**, 4874.
- ²² D. Ensign, M. Young, T. Douglas, *Inorg. Chem.* 2004, **43**, 3441.
- ²³ V. Nikandrov, C. Gratzel, J. Moser, M. Gratzel, *J. Photochem. Photobiol. B* 1997, **41**, 83.
- ²⁴ T. Rakshit, R. Mukhopadhyay, *Langmuir* 2011, **27**, 9681.
- ²⁵ R. Hilton, B. Zhang, L. Martineau, G. Watt, R. Watt, *J. Inorg. Biochem.* **2012**, *108*, 8.
- ²⁶ J. Colton, S. Erickson, T. Smith, R. Watt, *Nanotechnology* 2014, **25**, 135703.
- ²⁷ M. Joo, G. Tourillon, D. Sayers, E. Theil, *Biol. Met.* 1990, **3**, 171.
- ²⁸ R. Hilton, *Ph.D. Thesis, Brigham Young University* **2011**.
- ²⁹ M. Moss, M. Mellon, *Ind. Eng. Chem. Anal. Ed.* 1942, **14**, 862.
- ³⁰ O. Lowry, N. Rosebrough, A. Farr, R. Randall, *J. Biol. Chem.* 1951, **193**, 265.
- ³¹ R. Hilton, N. David Andros, R. Watt, *Biometals.* 2012, **25**, 259.
- ³² J. Johnson, M. Cannon, R. Watt, R. Frankel, G. Watt, *Biochemistry* 1999, **38**, 6706.



The substitution of alternate anions into the iron core of ferritin alters the mineral and changes the band gap of the resulting materials.
227x102mm (300 x 300 DPI)